

Removal of organic dyes from aqueous solutions using a graphene-containing sorbent based on activated rapeseed biochar: kinetics and isotherms

© Alexey N. Timirgaliev^a, Irina V. Burakova^a✉, Sofya O. Rybakova^a, Oksana A. Ananyeva^a, Vladimir O. Yarkin^a, Tatyana S. Kuznetsova^a, Ali H. K. Kadum^a, Alexander E. Burakov^a

^a Tambov State Technical University,
Bld. 2, 106/5, Sovetskaya St., Tambov, 392000, Russian Federation

✉ iris_tamb68@mail.ru

Abstract: The paper deals with the development of a graphene-containing sorbent material based on activated rapeseed biochar. The physicochemical properties of the sorbent and features of its morphological structure were determined. The nanocomposite was found to have amorphous properties with a graphene-like structure. The morphological analysis confirmed the formation of internal carbon framework and external three-dimensional multilayer graphene structure, which is excellent for mass transfer between pollutants and adsorbent surface. The research also aimed to determine the important parameters of sorption of organic compounds, i.e. synthetic dyes Congo Red (CR) and Malachite Green (MG), on the developed material from aqueous solutions in a limited volume. According to the kinetic studies, the experimental sorption capacity of the material on MG was $1860 \text{ mg}\cdot\text{g}^{-1}$ (sorption time – 60 min) and $642 \text{ mg}\cdot\text{g}^{-1}$ on CR (sorption time – 15 min). The theoretical maximum adsorption capacity of the sorbent calculated by the Langmuir model reached values of $769.23 \text{ mg}\cdot\text{g}^{-1}$ for CR and $3333.33 \text{ mg}\cdot\text{g}^{-1}$ for MG. It is found that the extraction of dye molecules is controlled by the second-order reaction according to the pseudo-second-order model and proceeds mainly by a mixed-diffusion mechanism. The activation energy has a value of $0.01 \text{ kJ}\cdot\text{mol}^{-1}$ for CR molecules and $0.02 \text{ kJ}\cdot\text{mol}^{-1}$ for MG, confirming the physical mechanism of dye adsorption. The high efficiency of adsorption of organic dyes on graphene-containing sorption material based on activated rapeseed biochar was demonstrated, indicating the feasibility of its practical application in wastewater treatment.

Keywords: graphene oxide; activated carbon; biochar; rapeseed; synthetic dyes; Congo Red; Malachite Green; adsorption; kinetics; isotherms.

For citation: Timirgaliev AN, Burakova IV, Rybakova SO, Ananyeva OA, Yarkin VO, Kuznetsova TS, Kadum AHK, Burakov AE. Removal of organic dyes from aqueous solutions using a graphene-containing sorbent based on activated rapeseed biochar: Kinetics and isotherms. *Journal of Advanced Materials and Technologies*. 2024;9(3):177-187. DOI: 10.17277/jamt.2024.03.pp.177-187

Удаление органических красителей из водных растворов с помощью графенсодержащего сорбента на основе активированного рапсового биоугля: кинетика и изотермы

© А. Н. Тимиргалиев^a, И. В. Буракова^a✉, С. О. Рыбакова^a, О. А. Ананьева^a, В. О. Яркин^a, Т. С. Кузнецова^a, А. Х. К. Кадум^a, А. Е. Бураков^a

^a Тамбовский государственный технический университет,
ул. Советская, 106/5, пом. 2, Тамбов, 392000, Российская Федерация

✉ iris_tamb68@mail.ru

Аннотация: В статье разработан графенсодержащий сорбционный материал на основе активированного рапсового биоугля, определены физико-химические свойства сорбента и особенности его морфологического строения. Установлено, что наноккомпозит имеет аморфные характеристики с графеноподобной структурой. Морфологический анализ подтвердил образование внутреннего углеродного каркаса и внешней трехмерной многослойной графеновой структуры, которая превосходно подходит для массопереноса между загрязнителями

и поверхностью адсорбента. Также целью исследований являлось определение важных параметров сорбции органических соединений – синтетических красителей конго красного (КК) и малахитового зеленого (МЗ), на разработанном материале из водных растворов в ограниченном объеме. Согласно кинетическим исследованиям, экспериментальная сорбционная емкость материала по МЗ составила 1860 мг/г (время сорбции 60 мин) и 642 мг/г по КК (время сорбции 15 мин). Теоретическая максимальная адсорбционная емкость сорбента, рассчитанная по модели Ленгмюра, достигла значений 769,23 мг/г по КК и 3333,33 мг/г по МЗ. Обнаружено, что извлечение молекул красителей контролируется реакцией второго порядка согласно модели псевдо-второго порядка и проходит преимущественно по смешанно-диффузионному механизму. Энергия активации имеет значение 0,01 кДж/моль по молекулам КК и 0,02 кДж/моль для МЗ, что подтверждает физический механизм поглощения красителей. В целом, в работе показана высокая эффективность адсорбции органических красителей на графенсодержащем сорбционном материале на основе активированного рапсового биоугля, что позволяет говорить о целесообразности его практического применения при очистке сточных вод.

Ключевые слова: оксид графена; активированный уголь; биоуголь; рапс; синтетические красители; конго красный; малахитовый зеленый; адсорбция; кинетика; изотермы.

Для цитирования: Timirgaliev AN, Burakova IV, Rybakova SO, Ananyeva OA, Yarkin VO, Kuznetsova TS, Kadum ANK, Burakov AE. Removal of organic dyes from aqueous solutions using a graphene-containing sorbent based on activated rapeseed biochar: Kinetics and isotherms. *Journal of Advanced Materials and Technologies*. 2024;9(3): 177-187. DOI: 10.17277/jamt.2024.03.pp.177-187

Introduction

According to a recent World Health Organization (WHO) report, nearly 844 million people worldwide do not have access to safe drinking water [1]. Dye-containing wastewater from the textile industry poses an increasing risk to human life and aquatic organisms when discharged into various water bodies, as most of the types of dyes found in dyeing wastewater are toxic and carcinogenic [2]. In addition, these dyes interfere with light penetration and oxygen transport in water bodies [3].

Malachite Green (MG) and Congo Red (CR) together account for a significant proportion of the organic dyes produced and used annually that pose significant health risks. MG is known for its potential teratogenic and carcinogenic properties, which can cause damage to vital organs such as the liver, kidney and heart [4]. CR is classified as an anionic diazo dye and is one of the most commonly used dyes [5]. Unfortunately, decomposition of CR under anaerobic conditions leads to the formation of benzidine, a known human carcinogen [6]. It is therefore crucial to remove organic dyes that pollute the environment's water resources in order to mitigate their harmful effects on humans, flora and fauna.

In their study, Ohemeng-Boahen et al. [6] presented a number of approaches for the removal of dye molecules, including adsorption, coagulation-flocculation, co-deposition, membrane separation, ion exchange, and photo- and biodegradation. Adsorption is regarded as an efficacious method for the elimination of dyes from wastewater, due to its advantageous characteristics, including flexibility, operational simplicity and economic viability [7]. At present, a variety of adsorbents are employed for

the removal of dyes, including biochar, activated carbon composites, nanoparticles, polymers, resins, clays, minerals and biosorbents [8].

Among the range of available adsorbents, activated carbon is undoubtedly considered the most versatile for use in studies of dye removal due to its low cost, excellent adsorption capacity, environmental friendliness and good surface characteristics [7]. Biochar is a bioorganic biomass produced by carbonization of carbon-rich materials. The modern low-temperature biomass processing method is hydrothermal carbonization (HTC), which is considered a green technology because of the absence of harmful gas emissions. The distinctive feature of this process is the relatively mild conditions under which it is carried out, in comparison with the well-studied pyrolysis process [8–10].

Many scientific teams are engaged in the development of new sorbents. They demonstrate remarkable efficacy in removing organic dyes from liquids (Fig. 1).

Thus, a number of materials of different chemical nature have been used for MG adsorption, for example: activated carbon with zinc oxide decorated with plantain peel [11]; magnetic mesoporous core-shell nanostructure $Ni_{0.4}Fe_{2.6}O_4/(Fe, Ni)$ with carbon [12]; chemically activated biochar from Indian bael peel [13]; functionalized biochar from banana peel [14]; halloysite nanotubes [15]; β -cyclodextrin nanocomposite based on polymer with zinc ferrite nanofiller [16]. For CR removal the following are used: β -cyclodextrin polyurethane insoluble nanosponge modified with phosphorylated multi-walled carbon nanotubes and additionally decorated with titanium dioxide and silver nanoparticles [17];

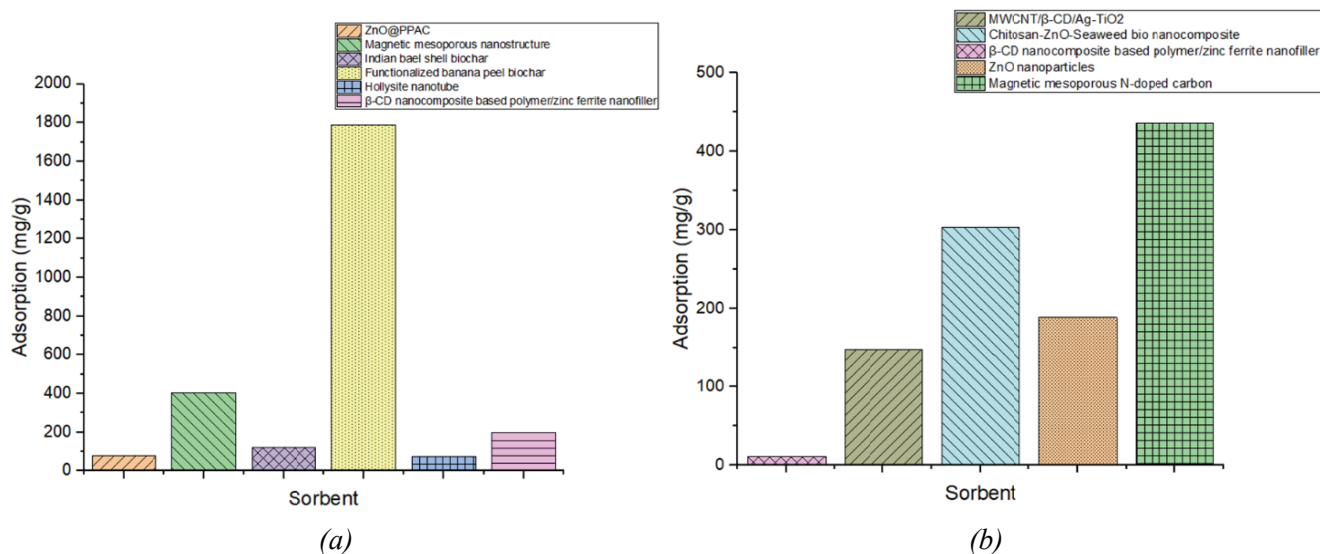


Fig. 1. Literature data on the sorption of MG (a) and CR (b) on different types of sorbents and their sorption capacity

bionanocomposite consisting of chitosan, zinc oxide, algae [18]; β -cyclodextrin nanocomposite based on polymer containing zinc ferrite nanofiller [16]; zinc oxide nanoparticles [19]; magnetic and mesoporous N-doped carbon [20].

The aim of the present work is to synthesize and evaluate the physicochemical properties of graphene-containing activated biochar based on vegetable waste from rapeseed processing and to determine the mechanisms of removal of organic contaminants – CR and MG dyes – using the developed material.

2. Materials and Methods

2.1. Material's synthesis

Rapeseed meal (originating from Tambov region, Russia) was used as a carbon source. The modifier was graphene oxide (GO) in the form of aqueous 1 wt. % suspension (NanoTechCenter LLC, Tambov). Biochar was obtained by hydrothermal carbonization in stainless steel autoclaves for 12 hours at 180 °C. The obtained hydrocoal was separated from the liquid by filtration. Further, the filtered material was carbonized in stages at 150, 500 and 750 °C for one hour at each temperature in argon atmosphere. The carbonized material was subjected to alkaline activation, for this purpose it was mixed with potassium hydroxide (KOH) in a mass ratio of 1:6. The process was carried out in an inert environment at 400 and 750 °C for one hour at each temperature. The resulting material was washed with distilled water on a filter to a neutral pH, and then incubated for 24 hours in concentrated hydrochloric acid (Russian Standard 3118-77). Then the biochar was washed again to neutral pH and dried at 110 °C to constant weight.



Fig. 2. Physical appearance of graphene-containing sorbent based on rapeseed

To obtain a nanocomposite sorbent, activated biochar was mixed with a suspension of GO to a homogeneous state (ratio 1.5:1) and then treated with ultrasound. The material was placed in autoclaves and incubated at 180 °C for 20 hours. In the next step, the composite was frozen to –30 °C in a lyophilic dryer (Scientz-10n, China), followed by lyophilization for 48 h, during which the solvent was removed by the freeze-drying. The final material was a spontaneously compacted product (see Fig. 2).

2.2. Analytical methods

Microphotographs were obtained using an AURIGA CrossBeam scanning electron microscope (SEM) with Inca X-Max 80 mm² EDS (Carl Zeiss Group, Germany). Thermo Scientific ARL Equinox 1000 (TechTrend Science Co., Ltd., Taiwan) ($\lambda = 0.1540562$ nm (copper anode) was used to identify

the crystal structure of the material. The orderliness of the carbon framework was evaluated by Raman spectroscopy on a DXR Raman Microscope instrument (Thermo Scientific Instruments Group, Waltham, USA) ($\lambda = 633$ nm). IR spectra were obtained on a Jasco FT/IR 6700 FTIR spectrometer (Jasco International Co., Ltd., Japan) in the frustrated total internal reflection mode.

2.3. Kinetic research

To determine the kinetic parameters of CR and MG adsorption, experiments were performed under static conditions; for this purpose, 0.01 g of nanocomposite was taken, the initial concentration of CR and MG dye solutions was $1500 \text{ mg}\cdot\text{L}^{-1}$, and the solution volume was 30 mL. The solutions were stirred for 5, 10, 15, 30, 60 and 90 min at 100 rpm and room temperature on a Multi Bio RS-24 rotator (Biosan) and then filtered.

2.4. Isotherm study

To plot adsorption isotherms, 0.01 g of nanocomposite was added to 30 mL of CR and MG dye solution with initial concentrations of 300, 500, 750, 750, 1000, 1200, and $1500 \text{ mg}\cdot\text{L}^{-1}$, shaken for 15 min for CR and 60 min for MG at 100 rpm and room temperature on a Multi Bio RS-24 programmable rotator (Biosan). In all sorption experiments, the amount of dye in the liquid phase before and after adsorption was determined spectrophotometrically (Ekros, St. Petersburg, Russia) at wavelengths of 612 and 709 nm for CR and MG, respectively.

3. Results and Discussion

3.1. Physicochemical properties and morphology of the graphene-containing sorbent

SEM images (Fig. 3) of the nanocomposite sorbent indicate that the material has a rather loose structure. The carbon backbone of the biochar is predominantly covered with graphene sheets. Individual aggregates of micrometer-sized graphene sheets are also found.

The IR spectrum of the nanocomposite (Fig. 4a) contains peaks indicating the presence of sorbed water (broad peak in the region of 3400 cm^{-1}), C–H bonds in alkyl fragments ($2924, 2854 \text{ cm}^{-1}$), C=O (1645 cm^{-1}), aromatic ring bonds at 1564 cm^{-1} , C–O (group of peaks in the region of $1100\text{--}1265 \text{ cm}^{-1}$), and phosphorus-containing compounds (873 cm^{-1}). The obtained data correlate well with the information on the chemical nature of carbon structures in the scientific literature [21–23].

According to Raman spectroscopy (Fig. 4b), the composition of the broad peak in the region $1000\text{--}1650 \text{ cm}^{-1}$ includes the *G* band (around 1590 cm^{-1}) and *D* band (at 1350 cm^{-1}). A second-order overtone of the *D* band, the *2D* band at 2670 cm^{-1} , can also be distinguished. Since the *2D* band arises from the two-phonon double resonance process, it is closely related to the zone structure of graphene layers [24]. The I_D/I_G ratio is > 1 , indicating a high content of sp^3 -hybridized carbon atoms in the material.

The X-ray spectrum (Fig. 5) shows blurred peaks at 26° and 47° , indicating the presence of 002 and 100 planes of graphene materials. The absence of sharp peaks in the spectra suggests that the nanocomposite has amorphous characteristics with graphene-like structure [23].

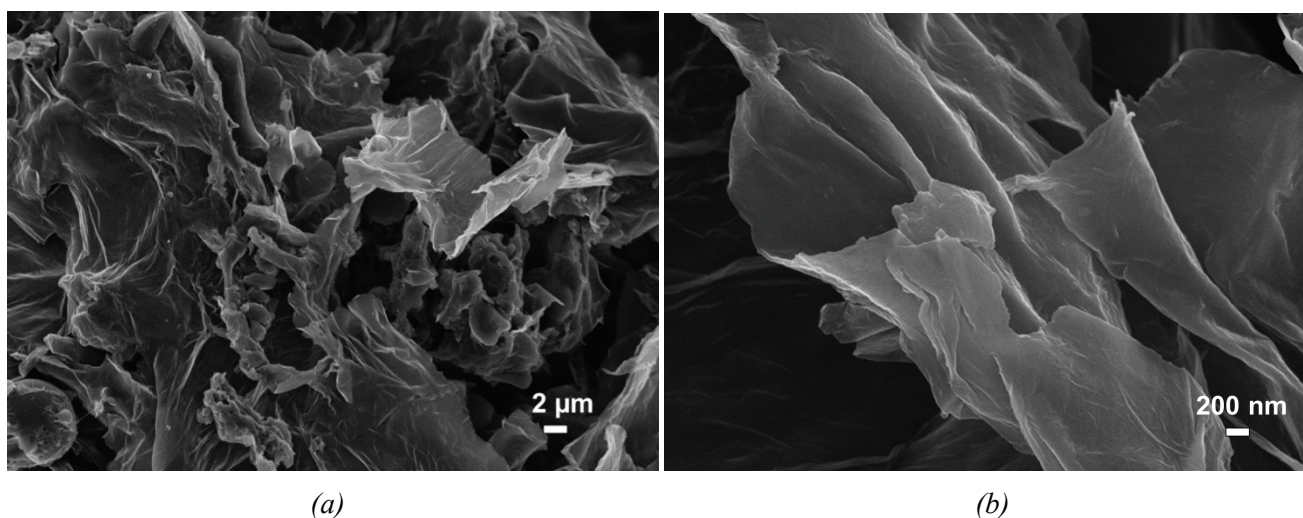


Fig. 3. SEM images of the nanocomposite: *a* – magnification $\times 5,000$; *b* – magnification $\times 50,000$

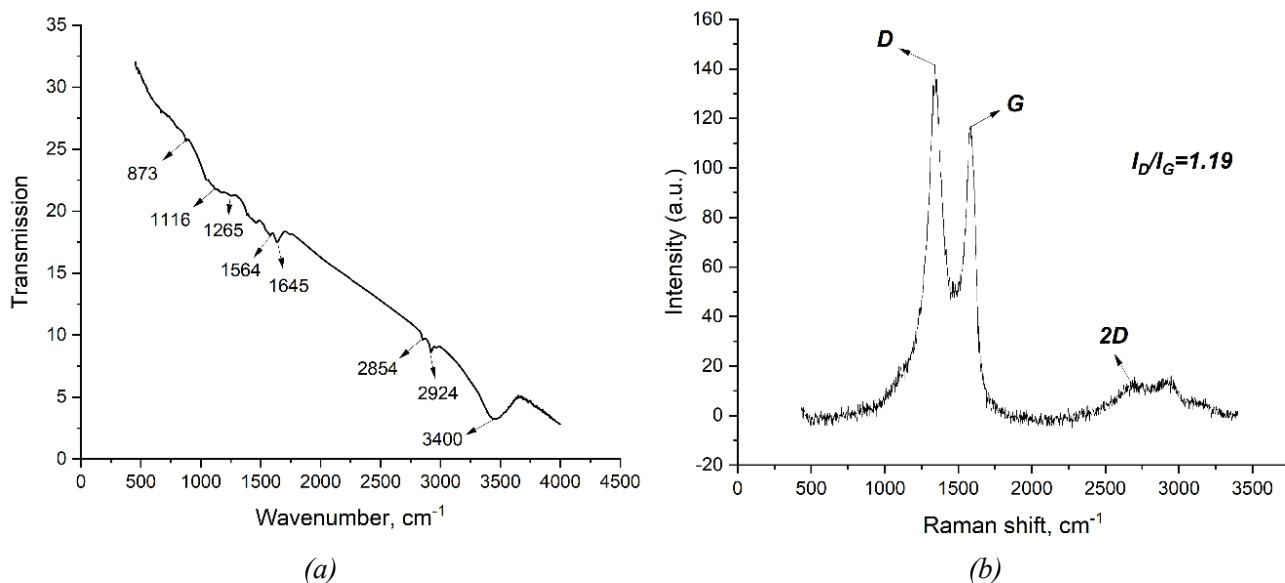


Fig. 4. FTIR (a) and Raman (b) spectra of the nanocomposite from rapeseed plant waste

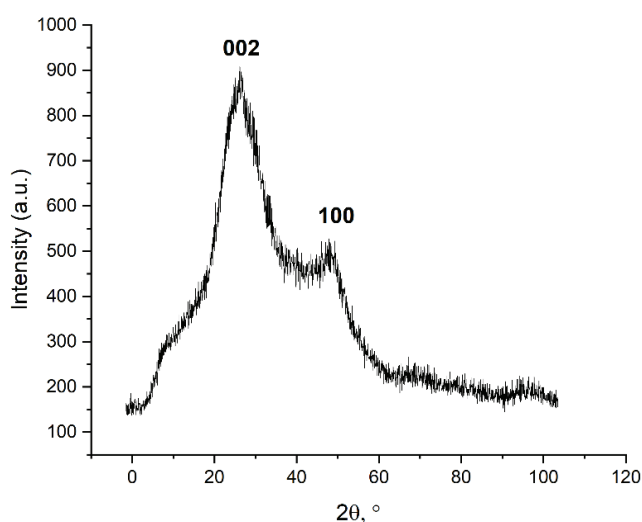


Fig. 5. X-ray diffraction pattern of the nanocomposite from rapeseed plant waste

3.2. Sorption kinetics of organic dyes

Based on the experimental results, the kinetic dependencies of the adsorption of CR and MG on the developed nanocomposite were plotted (Fig. 6a). The experimental values of the adsorption capacity of the material with respect to MG were $1860 \text{ mg}\cdot\text{g}^{-1}$ and $642 \text{ mg}\cdot\text{g}^{-1}$ for CR. It should be noted that the equilibrium of the adsorption process for CR adsorption is reached in 15 min. The extraction of MG is slower – saturation of the sorbent is reached in 60 min.

The kinetic analysis identifies the mechanism of adsorption and the factor determining its rate. The experimental data were analyzed using pseudo-first order, pseudo-second order, Elovich and

intraparticle diffusion models. The equations of these models are given in Table 1.

The pseudo-first and pseudo-second order models allow the determination of the pollutant uptake rate – the values of the sorption rate constants k_1 and k_2 . The pseudo-first order model characterises the processes occurring during the initial period of sorption and the pseudo-second order model describes the extraction mechanism for the entire period. The theoretical equation of intraparticle diffusion takes into account the rate of the internal mass transfer stage, i.e. the diffusion of sorbate in the pores of the sorbent with a spherical particle shape. In this case, if the graph of the dependence of Q_t on $t^{1/2}$ passes through the origin, intraparticle diffusion is the rate-controlling stage. The Elovich model suggests the presence of chemical heterogeneity of the sorbent surface, which favors chemical adsorption. When the experimental data are described by this equation, the adsorption process is chemical in nature [25].

Table 2 summarizes the results of the mathematical evaluation of the experimental kinetic data.

It was found (Fig. 6, Table 2) that the adsorption of MG and CR dye molecules is satisfactorily described by the pseudo-second-order and intraparticle diffusion models. The correlation of the experimental data according to the pseudo-second-order model (Fig. 6c) for CR sorption is $R^2 = 0.9999$ with the value of $Q_e = 667 \text{ mg}\cdot\text{g}^{-1}$. For MG molecules, $Q_e = 2000 \text{ mg}\cdot\text{g}^{-1}$ with $R^2 = 0.9966$. The theoretical value of Q_e by the pseudo-second-order model for both dyes is very close to the sorption capacity obtained experimentally.

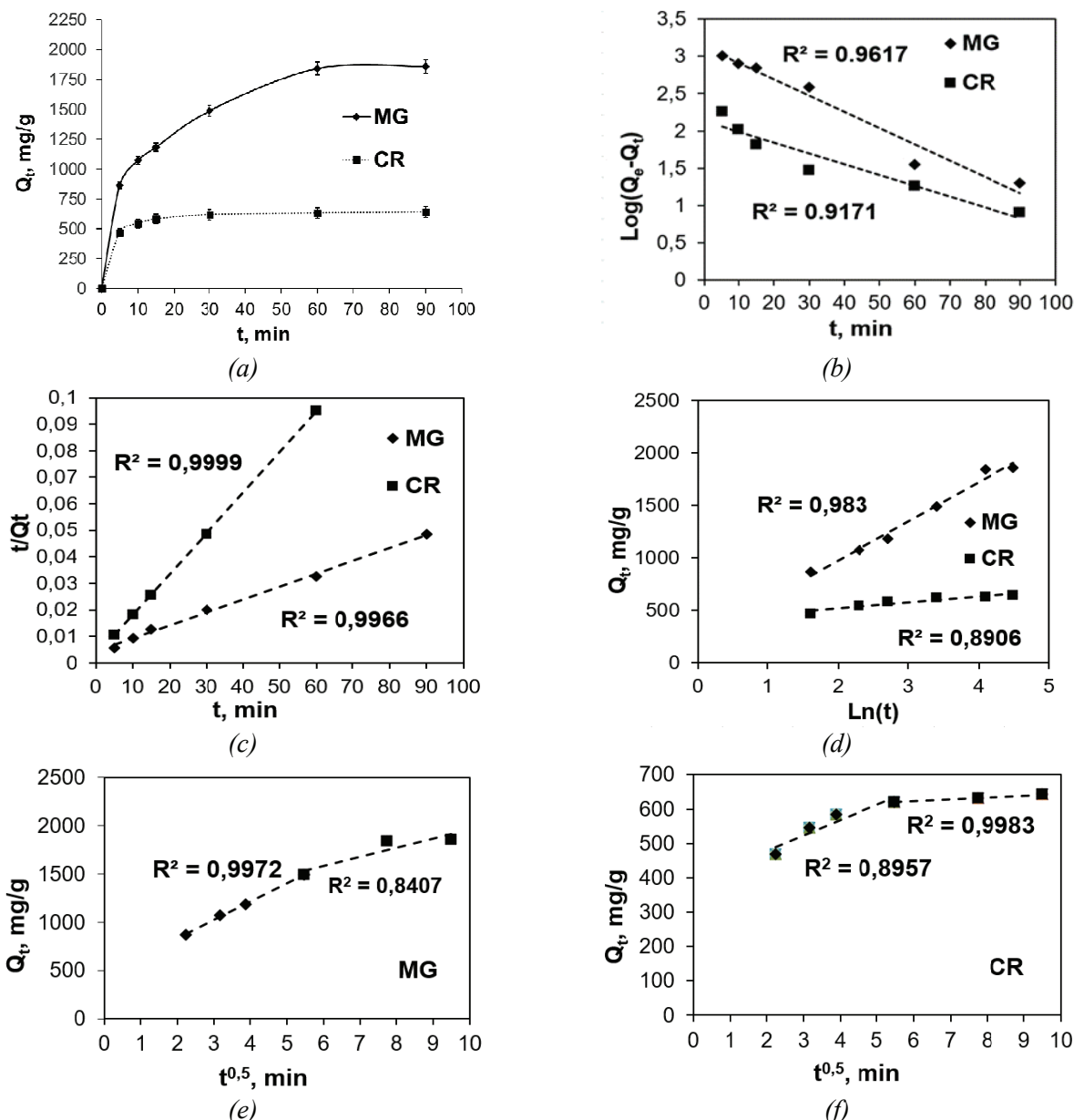


Fig. 6. Adsorption kinetics of CR and MG molecules on the nanocomposite (a), linearized forms of kinetic dependences by pseudo-first (b) and pseudo-second-order (c); Elovich (d); intraparticle diffusion (e, f) models

Table 1. Equations and parameters of different kinetic models [22]

| Model | Parameters |
|--|--|
| Pseudo-first-order model $\ln(Q_e - Q_t) = \ln Q_e - k_1 t$ | Q_e and Q_t ($\text{mg} \cdot \text{g}^{-1}$) are the amount of lead ions adsorbed at equilibrium and at any time t (min), respectively; k_1 is the rate constant of the pseudo-first-order (min^{-1}) equation |
| Pseudo-second-order model $\frac{t}{Q_t} = \frac{1}{k_2 Q_e^2} + \frac{t}{Q_e}$ | k_1 ($\text{g} \cdot (\text{mg} \cdot \text{min})^{-1}$) is the rate constant of the pseudo-second-order equation |
| Elovich model $Q_t = \frac{1}{\beta} \ln(1 + \alpha \beta t)$ | α ($\text{mg} \cdot \text{g}^{-1} \cdot \text{min}$) is the initial adsorption rate; β ($\text{g} \cdot \text{mg}^{-1}$) is the adsorption constant related to the degree of surface coverage and the activation energy of chemisorptions |
| Intraparticle diffusion model $Q_t = k_{id} t^{1/2} + C$ | k_{id} ($\text{mg} \cdot \text{g}^{-1} \cdot \text{min}^{1/2}$) is the rate constant of intraparticle diffusion; C is a constant related to the boundary layer thickness at the surface of the sorbent particle |

Table 2. Kinetic parameters of organic dyes sorption

| Dye | Model parameters | | | | | |
|-----|--------------------|---------|--------|--|---------------|---------------|
| | Pseudo-first order | | | Pseudo-first order | | |
| | Q_e | k_1 | R^2 | Q_e | k_2 | R^2 |
| CR | 152.4 | 0.0332 | 0.9171 | 667 | 0.000776 | 0.9999 |
| MG | 1349.9 | 0.0502 | 0.9617 | 2000 | 0.000056 | 0.9966 |
| | Elovich equation | | | Intraparticle diffusion Step 1/Step 2 | | |
| | α | β | R^2 | k_{id} | C | R^2 |
| CR | 71517.1 | 0.0018 | 0.891 | 44.98/5.427 | 388.71/590.22 | 0.8957/0.9983 |
| MG | 1129.03 | 0.0043 | 0.983 | 189.77/95.37 | 454.55/1009.6 | 0.9972/0.8407 |

According to Fig. 6b, rather low values of the coefficients ($R^2 = 0.9171$; 0.9617) of the pseudo-first order model suggest a weak chemical interaction between the molecules of the CR and MG dyes and the functional groups of the nanocomposite. The Elovich model shows a low correlation with the experimental data, again suggesting that mainly physical adsorption takes place [26].

The Q_t vs. t dependence is not a straight line through the origin of the coordinates, indicating that internal diffusion is not the limiting stage of adsorption. This may be due to the difference in mass transfer rate at the initial and final stages of sorption, i.e. the adsorption of dye molecules has a mixed-diffusion character [25].

3.3. Isotherm study

There are many models that can be used to interpret sorption isotherms, but the usefulness and accuracy of a particular model depends on the

underlying assumptions, as no model works for all adsorption systems. Among these models, the Freundlich and Langmuir models are the most widely used [26, 27]. The Langmuir isotherm assumes that adsorption results in the formation of a monolayer of adsorbate on the adsorbent surface. In contrast, the Freundlich model describes multilayer adsorption with an exponential decrease in the energy distribution of the adsorbed centers [28] (Table 3).

The Temkin isotherm model allows the activity of the sorbent surface centers to be estimated, with the activity of each of them decreasing as a result of the appearance of a number of surface sorption complexes. The more such complexes, the more the initial activity of that center changes. Thus, the activity of each center decreases as the degree of surface coverage by adsorbate increases.

Table 3. Equations and parameters of different isotherm models [26–28]

| Model | Parameters |
|---|--|
| The Langmuir model $\frac{1}{Q_e} = \frac{1}{Q_{\max}} + \frac{1}{Q_{\max} K_L C_e}$ | Q_e (mg·g ⁻¹) is the amount of metal ions adsorbed at equilibrium; the Q_{\max} (mg·g ⁻¹) is the maximum adsorption under experimental conditions; C_e (mg·L ⁻¹) is the equilibrium concentration; K_L (L·mg ⁻¹) is a constant related to the adsorption rate |
| The Freundlich model $\lg Q_e = \frac{1}{n} \lg C_e + \lg k$ | k (mg·g ⁻¹ ·(L·mg ⁻¹)); $1/n$ are constants measuring adsorption capacity and intensity, respectively; n indicates how favorable the adsorption process is |
| The Temkin model $Q_e = B \ln(k_t) + B \ln(C_e)$ | k_t (L·mg ⁻¹) is an equilibrium coupling constant corresponding to the maximum binding energy; B (J·mol ⁻¹) is a constant related to the heat of adsorption |
| The Dubinin–Radushkevich model $\lg Q_e = \ln Q_{\max} - K_{ad} \varepsilon^2;$ $E = \frac{1}{\sqrt{-2k_{ad}}}$ | k_{ad} (mol ² ·kJ ⁻²) is the constant of Dubinin–Radushkevich isotherm; ε (kJ·mol ⁻¹) is the Polanyi potential reflecting the isothermal work of transfer of one mole of metal from the volume of equilibrium solution to the sorbent surface; E (kJ·mol ⁻¹) is the activation energy |

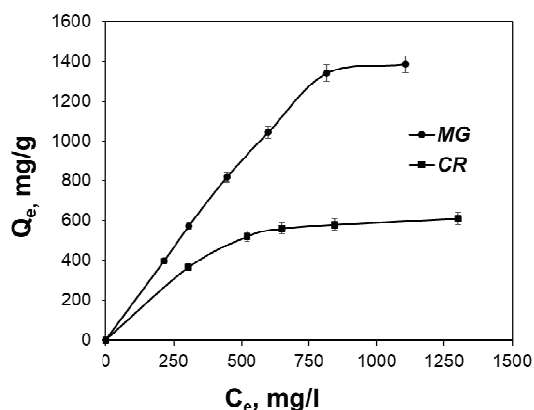


Fig. 7. Adsorption isotherms of CR and MG dyes on the nanocomposite

Using the Dubinin-Radushkevich model, calculations of activation energy are made, which determine the nature of interaction of pollutant forces with active centers. At activation energy values $E < 8 \text{ kJ}\cdot\text{mol}^{-1}$, physical adsorption takes place; at $8 < E < 16 \text{ kJ}\cdot\text{mol}^{-1}$, chemisorption takes place [29].

Fig. 7 shows the experimental adsorption isotherms of CR and MG dyes on the developed nanocomposite.

As a result of the mathematical processing of the experimental data, the dependences shown in Fig. 8 were obtained, which made it possible to determine such important adsorption parameters as maximum adsorption capacity, activation energy, etc. (see Table 4).

The experimental isotherm of MG sorption shows a good correlation with the theoretical data of the Dubinin-Radushkevich equation. The adsorption of CR is satisfactorily described by the Temkin model. At the same time, the activation energy of sorption of MG molecules was $0.02 \text{ kJ}\cdot\text{mol}^{-1}$ (Table 4). According to the calculated values, the maximum adsorption capacity of the nanocomposite according to the Langmuir model was $3333.33 \text{ mg}\cdot\text{g}^{-1}$ for MG and $769.23 \text{ mg}\cdot\text{g}^{-1}$ for CR. The value of the activation energy of sorption of CR molecules was $0.01 \text{ kJ}\cdot\text{mol}^{-1}$, which also corresponds to physical sorption in the case of removal of MG molecules.

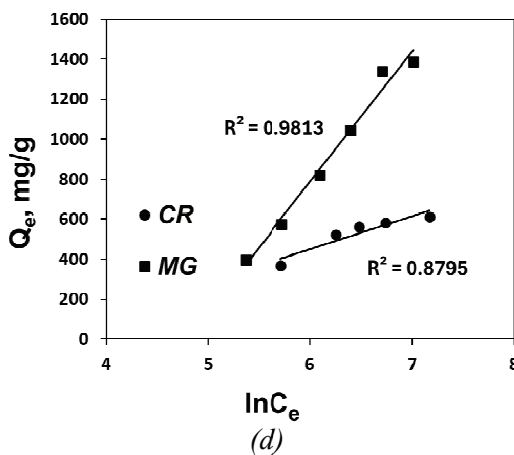
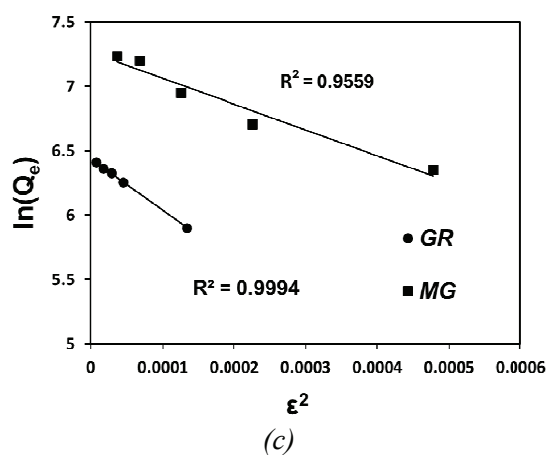
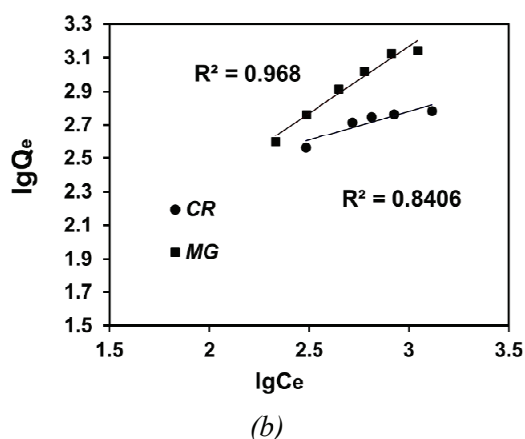
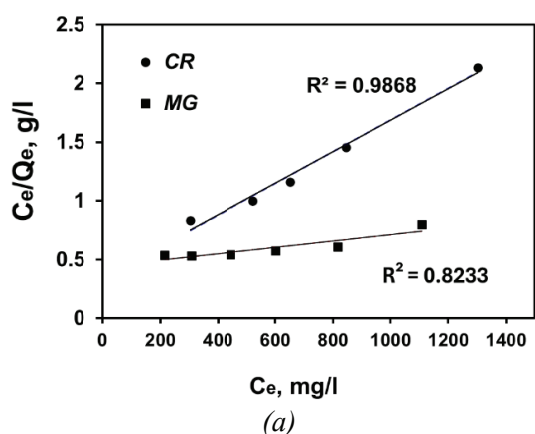


Fig. 8. Models of adsorption isotherms of CR and MG: a – Langmuir; b – Freundlich; c – Dubinin–Radushkevich; d – Temkin

Table 4. Sorption parameters of CR and MG molecules according to the equations of isotherms

| Dye | Model parameter | | | |
|-----|-----------------------------|------------|--------|--------|
| | <i>Langmuir</i> | | | |
| | K_L | Q_{\max} | R^2 | |
| CR | 0.0038 | 769.23 | 0.9868 | |
| MG | 0.0007 | 3333.33 | 0.8233 | |
| | <i>Freindlich</i> | | | |
| | n | $1/n$ | k | R^2 |
| CR | 2.891 | 0.3459 | 55.386 | 0.9868 |
| MG | 1.2596 | 0.7939 | 6.073 | 0.8233 |
| | <i>Dubinin–Radushkevich</i> | | | |
| | k_{ad} | Q_{\max} | E | R^2 |
| CR | 4053.6 | 629.34 | 0.01 | 0.9994 |
| MG | 2018.5 | 1438.12 | 0.02 | 0.9559 |
| | <i>Temkin</i> | | | |
| | k_t | B | R^2 | |
| CR | 0.0091 | 116.2 | 0.8795 | |
| MG | 0.0084 | 652.2 | 0.9813 | |

4. Conclusion

In this paper, the technique for obtaining a highly efficient sorbent material based on activated biochar from rapeseed waste modified with graphene oxide during hydrothermal carbonization has been developed. According to the results of the evaluation of the nanocomposite's properties, it was found that the material has a porous carbon framework, the surface of which is covered with sheets of graphene. X-ray diffraction analysis confirmed the formation of a graphene-like carbon structure of the sorbent. The authors studied the adsorption of synthetic organic dyes from aqueous solutions on the developed material. Kinetic and isothermal studies of adsorption of CR and MG dye molecules were carried out in static mode. It was found that the sorption equilibrium is reached in 60 min for MG and in 15 min for CR with sorption capacity values of $1860 \text{ mg}\cdot\text{g}^{-1}$ for MG and $642 \text{ mg}\cdot\text{g}^{-1}$ for CR. It was found that the sorption is satisfactorily described by the pseudo-second-order model and intraparticle diffusion, with diffusion into the sorbent pores not being a limiting factor. Both external and internal diffusion contribute to the total sorption rate of the dye molecules. Data from isothermal studies were processed using the Langmuir, Freundlich, Dubinin–Radushkevich and Temkin models. The calculated activation energy values confirm the physical mechanism of sorption.

5. Funding

The study was supported by the Russian Science Foundation grant No. 22-13-20074, <https://rscf.ru/project/22-13-20074/>.

6. Acknowledgments

This work was done using facilities of the shared access center “Production and application of multifunctional nanomaterials” (Tambov State Technical University).

7. Conflict of interests

The authors declare no conflict of interests.

References

1. Wutich A, Rosinger AY, Stoler J, Jepson W, et al. Measuring human water needs. *American Journal of Human Biology*. 2020;32(1):e23350. DOI:10.1002/ajhb.23350
2. Berradi M, Hsissou R, Khudhair M, Assouag M, et al. Textile finishing dyes and their impact on aquatic environs. *Heliyon*. 2019;5(11):e02711. DOI:10.1016/j.heliyon.2019.e02711
3. Peng X, Huang D, Odoom-Wubah T, Fu D, et al. Adsorption of anionic and cationic dyes on ferromagnetic ordered mesoporous carbon from aqueous solution: equilibrium, thermodynamic and kinetics. *Journal of Colloid and Interface Science*. 2014;430:272-282. DOI: 10.1016/j.jcis.2014.05.035

4. Eltaweil AS, Ali Mohamed H, Abd El-Monaem EM, El-Subruiti GM. Mesoporous magnetic biochar composite for enhanced adsorption of malachite green dye: characterization, adsorption kinetics, thermodynamics and isotherms. *Advanced Powder Technology*. 2020;31(3): 1253-1263. DOI:10.1016/j.appt.2020.01.005
5. Wang X, Xu Q, Zhang L, Pei L, et al. Adsorption of methylene blue and congo red from aqueous solution on 3d mxene/carbon foam hybrid aerogels: a study by experimental and statistical physics modeling. *Journal of Environmental Chemical Engineering*. 2023;11(1):109206. DOI:10.1016/j.jece.2022.109206
6. Ohemeng-Boahen G, Sewu DD, Tran HN, Woo SH. Enhanced adsorption of congo red from aqueous solution using chitosan/hematite nanocomposite hydrogel capsule fabricated via anionic surfactant gelation. *Colloids and Surfaces A: Physicochemical and Engineering Aspects*. 2021;625:126911. DOI:10.1016/j.colsurfa.2021.126911
7. Boretti A, Rosa L. Reassessing the projections of the world water development report. *Npj Clean Water*. 2019;2(1):15. DOI:10.1038/s41545-019-0039-9
8. Pichel N, Vivar M, Fuentes M. The problem of drinking water access: a review of disinfection technologies with an emphasis on solar treatment methods. *Chemosphere*. 2019;218:1014-1030. DOI:10.1016/j.chemosphere.2018.11.205
9. Sabzehmeidani MM, Mahnaee S, Ghaedi M, Heidari H, et al. Carbon based materials: a review of adsorbents for inorganic and organic compounds. *Materials Advances*. 2021;2(2):598-627. DOI:10.1039/D0MA00087F
10. Khan TA, Saud AS, Jamari SS, Rahim MHA, et al. Hydrothermal carbonization of lignocellulosic biomass for carbon rich material preparation: a review. *Biomass and Bioenergy*. 2019;130:105384. DOI:10.1016/j.biombioe.2019.105384
11. Dada AO, Inyinbor AA, Tokula BE, Bayode AA, et al. Zinc oxide decorated plantain peel activated carbon for adsorption of cationic malachite green dye: mechanistic, kinetics and thermodynamics modeling. *Environmental Research*. 2024;252:119046. DOI:10.1016/j.envres.2024.119046
12. Liu Y, Wei S, Kamali BE, Ege D, et al. Ni_{0.4}Fe_{2.6}O₄/(Fe, Ni)-carbon core-shell magnetic mesoporous nanostructure for efficient adsorption and photocatalytic degradation of malachite green from wastewater. *Journal of Water Process Engineering*. 2024;59:105019. DOI:10.1016/j.jwpe.2024.105019
13. Das T, Debnath A, Manna MS. Adsorption of malachite green by aegle marmelos-derived activated biochar: novelty assessment through phytotoxicity tests and economic analysis. *Journal of the Indian Chemical Society*. 2024;101(9):101219. DOI:10.1016/j.jics.2024.101219
14. Chen L, Mi B, He J, Li Y, et al. Functionalized biochars with highly-efficient malachite green adsorption property produced from banana peels via microwave-assisted pyrolysis. *Bioresource Technology*. 2023;376: 128840. DOI:10.1016/j.biortech.2023.128840
15. Altun T, Ecevit H. Adsorption of malachite green and methyl violet 2b by halloysite nanotube: batch adsorption experiments and box-behnken experimental design. *Materials Chemistry and Physics*. 2022;291: 126612. DOI:10.1016/j.matchemphys.2022.126612
16. Sirach R, Dave PN. β -cyclodextrin polymer/zinc ferrite nanocomposite: synthesis, characterization, and adsorption application for the removal of malachite green and Congo red. *Journal of Hazardous Materials Advances*. 2023;10:100300. DOI:10.1016/j.hazadv.2023.100300
17. Leudjo Taka A, Fosso-Kankeu E, Pillay K, Yangkou Mbianda X. Metal nanoparticles decorated phosphorylated carbon nanotube/cyclodextrin nanosponge for trichloroethylene and Congo red dye adsorption from wastewater. *Journal of Environmental Chemical Engineering*. 2020;8(3):103602. DOI:10.1016/j.jece.2019.103602
18. Gopalakrishnan S, Kannan P, Balasubramani K, Rajamohan N, et al. Sustainable remediation of toxic Congo red dye pollution using bio based carbon nanocomposite: modelling and performance evaluation. *Chemosphere*. 2023;343:140206. DOI: 10.1016/j.chemosphere.2023.140206
19. Abegunde SM, Olasehinde EF, Adebayo MA. Green synthesis of ZnO nanoparticles using nauclea latifolia fruit extract for adsorption of Congo red. *Hybrid Advances*. 2024;5:100164. DOI: 10.1016/j.hybadv.2024.100164
20. Rao R, Huang Y, Zhang H, Hu C, et al. A simple melamine-assisted cellulose pyrolysis synthesis of magnetic and mesoporous n-doped carbon composites with excellent adsorption of Congo red. *Separation and Purification Technology*. 2024;347:127678. DOI:10.1016/j.seppur.2024.127678
21. Li N, Yan X, Dai W, Lv B, et al. Adsorption properties and mechanism of sepiolite to graphene oxide in aqueous solution. *Arabian Journal of Chemistry*. 2023;16(4):104595. DOI:10.1016/j.arabjc.2023.104595
22. Ali I, Burakov AE, Burakova IV, Kuznetsova TS, et al. Facile and economic preparation of graphene hydrothermal nanocomposite from sunflower waste: kinetics, isotherms and thermodynamics for Cd(II) and Pb(II) removal from water. *Journal of Molecular Liquids*. 2024;407:125179. DOI:10.1016/j.molliq.2024.125179
23. Adel M, El-Maghraby A, El-Shazly O, El-Wahidy EWF, Mohamed MAA. Synthesis of few-layer graphene-like nanosheets from glucose: New facile approach for graphene-like nanosheets large-scale production. *Journal of Materials Research*. 2016;31:455-467. DOI:10.1557/jmr.2016.25
24. Ni Z, Wang Y, Yu T, Shen Z. Raman spectroscopy and imaging of graphene. *Nano Research*. 2008;1(4):273-291. DOI: 10.1007/s12274-008-8036-1
25. Qiu H, Lv L, Pan B, Zhang Q, et al. Critical review in adsorption kinetic models. *Journal of Zhejiang University-SCIENCE A*. 2009;10(5):716-724. DOI:10.1631/jzus.A0820524
26. Naghizadeh A, Ghasemi F, Derakhshani E, Shahabi H. Thermodynamic, kinetic and isotherm studies of sulfate removal from aqueous solutions by graphene and

graphite nanoparticles. *Desalination and Water Treatment*. 2017;80:247-254. DOI:10.5004/dwt.2017.20891

27. Vigdorowitsch M, Pchelintsev A, Tsygankova L, Tanygina E. Freundlich isotherm: an adsorption model complete framework. *Applied Sciences*. 2021;11(17):8078. DOI:10.3390/app11178078

28. Kadum AHK, Burakova IV, Mkrtchyan ES, Ananyeva OA, et al. Sorption kinetics of organic dyes methylene blue and malachite green on highly porous

carbon material. *Journal of Advanced Materials and Technologies*. 2023;8(2):130-140. DOI:10.17277/jamt.2023.02.pp.130-140

29. Hameed BH, Tan IAW, Ahmad AL. Adsorption isotherm, kinetic modeling and mechanism of 2,4,6-trichlorophenol on coconut husk-based activated carbon. *Chemical Engineering Journal*. 2008;144(2):235244. DOI: 10.1016/j.cej.2008.01.028

Information about the authors / Информация об авторах

Alexey N. Timirgaliev, Master's Degree Student, Tambov State Technical University (TSTU), Tambov, Russian Federation; ORCID 0009-0006-5030-3677; e-mail: timirgaliev31@mail.ru

Irina V. Burakova, Cand. Sc. (Eng.), Associate Professor, TSTU, Tambov, Russian Federation; ORCID 0000-0003-0850-9365; e-mail: iris_tamb68@mail.ru

Sofya O. Rybakova, Student, TSTU, Tambov, Russian Federation; e-mail: sofarybackova@yandex.ru

Oksana A. Ananyeva, Postgraduate, TSTU, Tambov, Russian Federation; ORCID 0000-0002-1188-9402; e-mail: oksana.a9993471@gmail.com

Vladimir O. Yarkin, Master's Degree Student, TSTU, Tambov, Russian Federation; ORCID 0009-0001-2185-0149; e-mail: sttstu90@gmail.com

Tatyana S. Kuznetsova, Cand. Sc. (Eng.), Senior Lecturer, TSTU, Tambov, Russian Federation; ORCID 0000-0001-6508-2092; e-mail: kuznetsova-t-s@yandex.ru

Ali H. K. Kadum, Postgraduate, TSTU, Tambov, Russian Federation; e-mail: ali_strong_2010@yahoo.com

Alexander E. Burakov, Cand. Sc. (Eng.), Associate Professor, TSTU, Tambov, Russian Federation; ORCID 0000-0003-4871-3504; e-mail: m-alex1983@yandex.ru

Тимиргалиев Алексей Николаевич, магистрант, Тамбовский государственный технический университет (ТГТУ), Тамбов, Российская Федерация; ORCID 0009-0006-5030-3677; e-mail: timirgaliev31@mail.ru

Буракова Ирина Владимировна, кандидат технических наук, доцент, ТГТУ, Тамбов, Российская Федерация; ORCID 0000-0003-0850-9365; e-mail: iris_tamb68@mail.ru

Рыбакова Софья Олеговна, студент, ТГТУ, Тамбов, Российская Федерация; e-mail: sofarybackova@yandex.ru

Ананьева Оксана Альбертовна, аспирант, ТГТУ, Тамбов, Российская Федерация; ORCID 0000-0002-1188-9402; e-mail: oksana.a9993471@gmail.com

Яркин Владимир Олегович, магистрант, ТГТУ, Тамбов, Российская Федерация; ORCID 0009-0001-2185-0149; e-mail: sttstu90@gmail.com

Кузнецова Татьяна Сергеевна, кандидат технических наук, старший преподаватель, ТГТУ, Тамбов, Российская Федерация; ORCID 0000-0001-6508-2092; e-mail: kuznetsova-t-s@yandex.ru

Кадум Али Хуссейн Кадум, аспирант, ТГТУ, Тамбов, Российская Федерация; e-mail: ali_strong_2010@yahoo.com

Бураков Александр Евгеньевич, кандидат технических наук, доцент, ТГТУ, Тамбов, Российская Федерация; ORCID 0000-0003-4871-3504; e-mail: m-alex1983@yandex.ru

Received 19 June 2024; Accepted 26 July 2024; Published 22 October 2024



Copyright: © Timirgaliev AN, Burakova IV, Rybakova SO, Ananyeva OA, Yarkin VO, Kuznetsova TS, Kadum AHK, Burakov AE, 2024. This article is an open access article distributed under the terms and conditions of the Creative Commons Attribution (CC BY) license (<https://creativecommons.org/licenses/by/4.0/>).